CONF-820675--2

BNL 31597

BNL--31597

OG 642

DE82 019449

Talk presented at
International Neutrino 1982 Conference
Balaton, Hungary 6/14/82 - 6/19/82

MASTER

Preliminary Results on $\nu_\mu + e^- \rightarrow \nu_\mu + e^-$

N.J. Baker, P.L. Connolly, S.A. Kahn, H.G. Kirk,
M.J. Murtagh, R.B. Palmer, N.P. Samios and M. Tanaka
Brookhaven National Laboratory, Upton, NY 11973

and

C. Baltay, M. Bregman, D. Caroumbalis, L.D. Chen,
H. French, M. Hibbs, R. Hylton, P. Igo-Kemenes, J.T. Liu,
J. Okamitsu, G. Ormazabal, R.D. Schaffer, K. Shastri, J. Spitzer
Columbia University, New York, NY 10027

presented by N.J. Baker

Talk given at
International Neutrino 1982 Conference
Balaton, Hungary 6/14/82-6/19/82

PRELIMINARY RESULTS ON $\nu_\mu + e^- \rightarrow \nu_\mu + e^-$

N.J. Baker, P.L. Connolly, S.A. Kahn, H.G. Kirk,
M.J. Murtagh, R.B. Palmer, N.P. Samios and M. Tanaka
Brookhaven National Laboratory, Upton, NY 11973

and

C. Baltay, M. Bregman, D. Caroumbalis, L.D. Chen,
H. French, M. Hibbs, R. Hylton, P. Igo-Kemenes, J.T. Liu
J. Okamitsu, G. Ormazabal, R.D. Schaffer, K. Shastri, J. Spitzer
Columbia University, New York, NY 10027

presented by N.J. Baker

ABSTRACT

We present here preliminary results on a recent experiment on $\nu_\mu - e^-$ elastic scattering. A brief review of the Glashow-Salam-Weinberg theory is given, indicating how the measurement of the total cross section gives rise to an ambiguous solution for $\sin^2 \Theta_w$, and showing how the differential cross section can be used to resolve the ambiguity. The experimental configuration and the extraction of the signal are described. The data are compared with those from our previous experiment, and relevant distributions from the combined data sample are presented. The differential cross section is examined in an attempt to resolve the ambiguity in $\sin^2 \Theta_w$, the lower value of $\sin^2 \Theta_w = 0.20$ being favored.

The differential cross section for $\nu_\mu - e^-$ elastic scattering is given by:

$$\frac{d\,\sigma_\nu}{d\,E_e} = \frac{G^2 M_e}{2\,\pi}\left[(g_V + g_A)^2 + (g_V - g_A)^2 \left(1 - \frac{E_e}{E_\nu}\right)^2 - (g_V{}^2 - g_A{}^2)\frac{M_e\,E_e}{E_\nu{}^2}\right]$$

where E_ν = incident neutrino energy; E_e, M_e = Energy, Mass of the scattered electron; and g_V, g_A are the vector, axial-vector couplings of the neutral current to the electron. At FNAL/SPS energies, $E_\nu >> M_e$ and the third term above can be neglected.

The total cross section is given by

$$\sigma_\nu = \frac{G^2 M_e E_\nu}{2\,\pi}\left[(g_V + g_A)^2 + (g_V - g_A)^2 / 3\right]$$

The kinematics of this reaction impose a further constraint on the scattered electrons:

$$E_e\,\Theta_e{}^2 \leq 2\,M_e$$

where Θ_e is the scattering angle (with respect to the incident neutrino) of the electron; e.g. for electrons of energy 2 GeV (the lower limit for electrons in this experiment), the scattering angle $\Theta_e \lesssim 22.6$ mrad. Hence interactions due to $\nu_\mu - e^-$ elastic scattering are characterised by the observation of a single electron at a very small angle to the incident neutrino beam direction.

In the standard model of Glashow-Salam-Weinberg,[1] the couplings g_V, g_A are parameterized by

$$g_V = 2\sin^2\Theta_w - \tfrac{1}{2} \quad : \quad g_A = -\tfrac{1}{2},$$

such that the cross sections become

$$\frac{d\,\sigma_\nu}{d\,E_e} = \frac{G^2 M_e}{2\,\pi}\left[(2\sin^2\Theta_w - 1)^2 + (2\sin^2\Theta_w)^2\left(1 - \frac{E_e}{E_\nu}\right)^2\right]$$

$$\sigma_\nu = \frac{G^2 M_e E_\nu}{2\,\pi}\left[\frac{16}{3}\sin^4\Theta_w - 4\sin^2\Theta_w + 1\right]$$

Fig. 1 displays the slope (σ/E_ν) for neutrinos and antineutrinos as a function of $\sin^2 \Theta_w$, together with the result from our previous experiment[2] ($\sigma/E_\nu = (1.8 \pm 0.8) * 10^{-42}\ cm^2\ GeV^{-1}$). As can be seen an ambiguous value for $\sin^2 \Theta_w$ is obtained; $\sin^2 \Theta_w = 0.20^{+0.16}_{-0.08}$ or $0.57^{+0.07}_{-0.17}$. Fig. 2 displays the electron energy spectra which would be observed in the FNAL wide-band neutrino beam corresponding to the two values of $\sin^2 \Theta_w$.

The experiment was conducted at FNAL using the 15' bubble chamber filled with a heavy (64% atomic) Neon/Hydrogen mixture, operating a 30 kG. magnetic field. The radiation length of 40 cm. affords excellent electron identification. The angular resolution on electron tracks is typically 4 mrad, while the energy resolution is 10% at 2 GeV, and 15% at 20 GeV. The beam used in this experiment was the single horn focussed wideband neutrino beam producing a neutrino energy spectrum which extends from a few GeV to over 200 GeV, peaking at 25 GeV. In our previous experiment a two horn focussed beam was employed.

The data was selected via a two step process; firstly a dedicated scan to collect all unassociated electro-magnetic showers in the forward direction; and secondly the separation of the showers into electrons, positrons and photons ($\gamma \rightarrow e^+ e^-$). In the dedicated scan, the following event types were recorded:

1) All unassociated single electrons/positrons/photons within 30° of the beam direction (This large angle was selected, to avoid any losses caused by apparent distortions due to the optics).

2) Any low multiplicity interactions, in which there were any electron/positron and no more than two hadrons (excluding proton stubs due to nuclear breakup). These events are used in determining the background due to the reaction $\nu_e\, n \rightarrow e^- p$, in which the proton has too low an energy to be observed.

For a track to be considered as an electron/positron, it had to be identified by two or more of the usual signatures; converted bremstrahlung; annihilation; spiralization; large trident; or sudden curvature change. All events with an electron/positron having an energy greater than 2 GeV and within 52 mrad (3°) of the beam direction were considered by physicists in the second step.

The aim of the second step was to select single electrons/positrons while rejecting photons. An event was defined to be a single electron/positron, if there was no visible radiation on a negative/positive track, before there was observable curvature, so that the event clearly had a single track at the origin. If there was visible radiation on the track before curvature, the track was still considered as a single electron if (a) the fastest track coming from the confused region was negative, (b) the energy of the fastest positron was less than one quarter of the energy of the fastest electron and (c) the energy of the second fastest electron was greater than one tenth of the energy of the fastest positron. Condition (b) removes fast symmetric pairs and condition (c) removes asymmetric pairs with a delta near the origin. The losses caused by these conditions (an electron radiating more than one quarter of its energy into a highly asymmetric pair before the original electron had observable curvature) is calculated to be 3%

The data, from a single scan, is shown in Table 1, together with the data from the previous experiment and the combined total. The data are directly comparable, since each experiment had approximately the same flux of neutrinos, and from an initial estimate of the scanning efficiency, the single scan efficiency in the new experiment is equal to the overall scanning efficiency in the previous experiment. Clearly the new data are very consistent with the previous results. Fig. 3 displays the scatter plot of the electron energy E_e vs. the scattering angle Θ_e for all the single electron events. All the events are consistent with the kinematics of $\nu_\mu - e^-$ elastic scattering. Fig. 4 displays the variable $E\Theta^2$ for (a) the single electrons, (b) the single positrons; and (c) the isolated photons. The single electrons peak sharply, while the single positrons and isolated photons are more uniformly distributed.

The major background to the single electron signal arises from the reaction $\nu_e\, n \rightarrow e^-\, p$, in which the proton has such low energy that it is unobserved. The background due to this process is estimated at 6%. A further 1% background arises from asymmetric photons whose kinematics are consistent with $\nu_\mu - e^-$ elastic scattering.

The observed electron energy spectrum is shown in Fig. 5, together with the predicted spectrum corresponding to the two values of $\sin^2 \Theta_w$ determined in our previous experiment. The data appears to be in better agreement with the lower value for $\sin^2 \Theta_w$. In general the measurement of electrons in heavy liquid tends to underestimate the true electron energy. A mismeasurement of the electron energy would soften the energy spectrum, causing the higher value for $\sin^2 \Theta_w$ to be favored. This effect is not observed in our data.

In conclusion, we have approximately doubled the size of our previous data sample, the new data being very consistent with previous data. The observed electron energy spectrum from the combined data sample appears to favor the value of $\sin^2 \Theta_w = 0.20$ over $\sin^2 \Theta_w = 0.57$.

The determination of the scanning efficiency from a rescan of the film and a complete calculation of the background and losses will allow a precise measurement of the total cross section and $\sin^2 \Theta_w$. This research supported in part by the U. S. Department of Energy under Contract No. DE-AC02-76CH00016 and by the National Science Foundation.

TABLE 1

Number of Observed Events

Event Type	This Experiment	Previous Experiment	Combined Total
Single electron	9	11	20
Single positron	5	4	9
Isolated photon	27	22	49
ν_e Quasi-elastic $e^- p$ (+ stubs)	17	22	39
Overall Scanning Efficiency		(78 ± 15)%	

Figure 1. The slope (σ/E_ν) of the total cross sections for neutrino and anti-neutrino elastic scattering on electrons, as a function of $\sin^2 \Theta_W$. The dashed line is the result obtained from our previous experiment.

Figure 2. The predicted electron energy spectrum, corresponding to $\sin^2 \Theta_W = 0.20$ and $\sin^2 \Theta_W = 0.57$ from F.N.A.L. wideband beam.

Figure 3. The scatter plot of electron energy E_e vs. scattering angle Θ_e for the 20 observed single electrons.

Figure 4. The variable $E\Theta^2$ for (a) single electrons (b) single positrons and (c) isolated photons.

Figure 5. The observed electron energy spectrum. Overlaid on this plot are the predicted spectra from Figure 2.

REFERENCES

1) Glashow, S.L., Nucl. Phys. 22 579 (1961).

Salam, A., in 'Elememtary Particle Theory' edited by N. Svartholm (Almquist and Wiskells, Stockholm, 1969), p. 367.

Weinberg, S., Phys. Rev. Lett. 19, 1264 (1967)
Phys. Rev. Lett. 27, 1688 (1971).

2) A. M. Cnops, et al., Phys. Rev. Lett. 41 357 (1978).

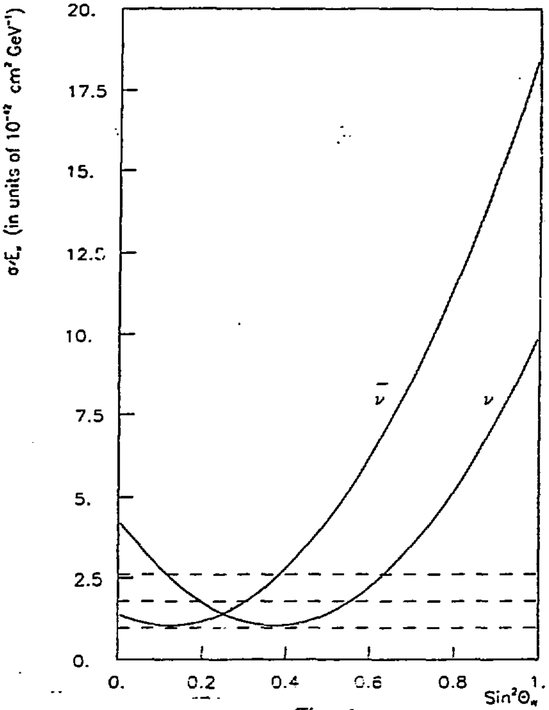

Fig. 1

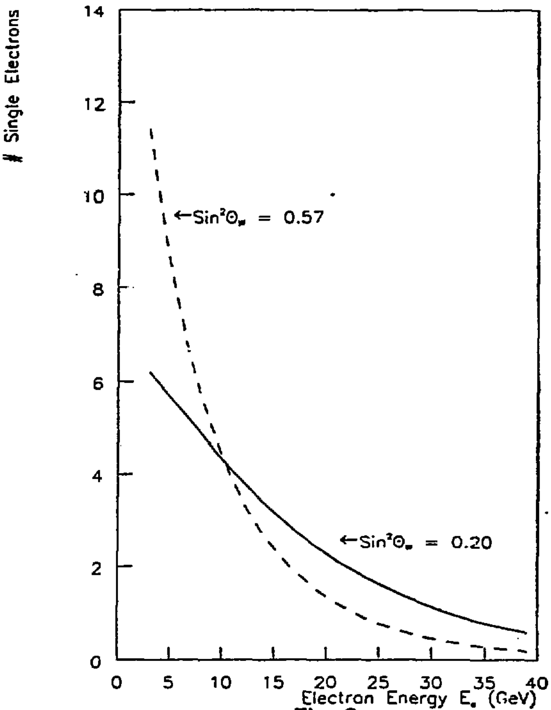

Fig. 2

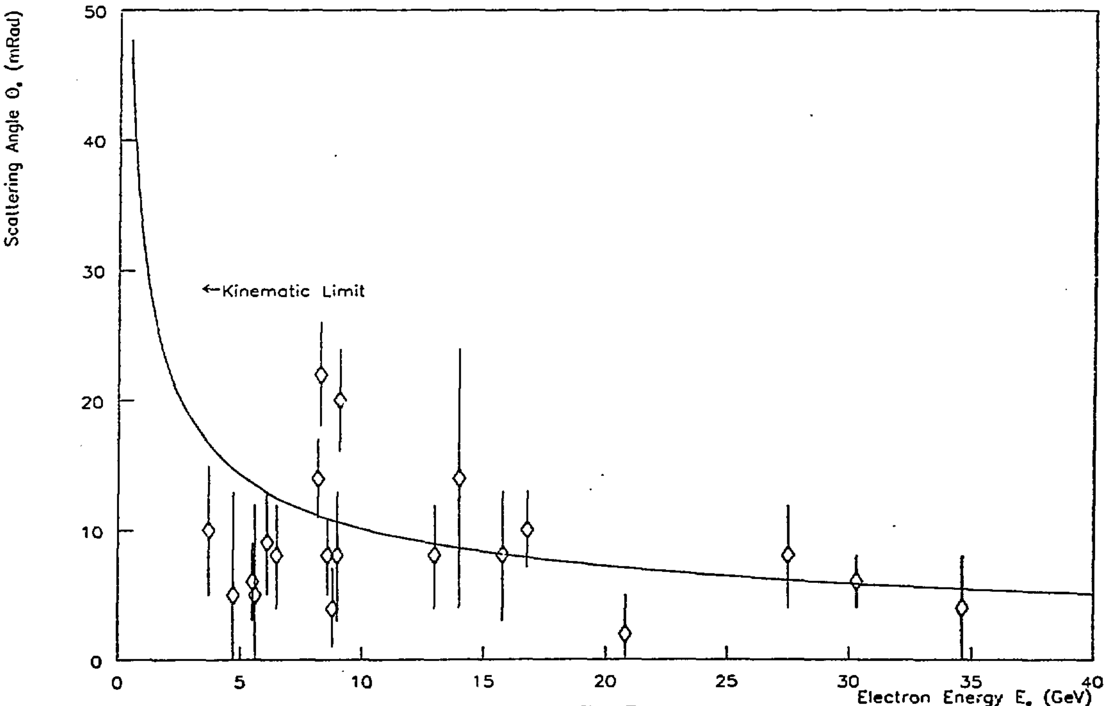

Fig. 3

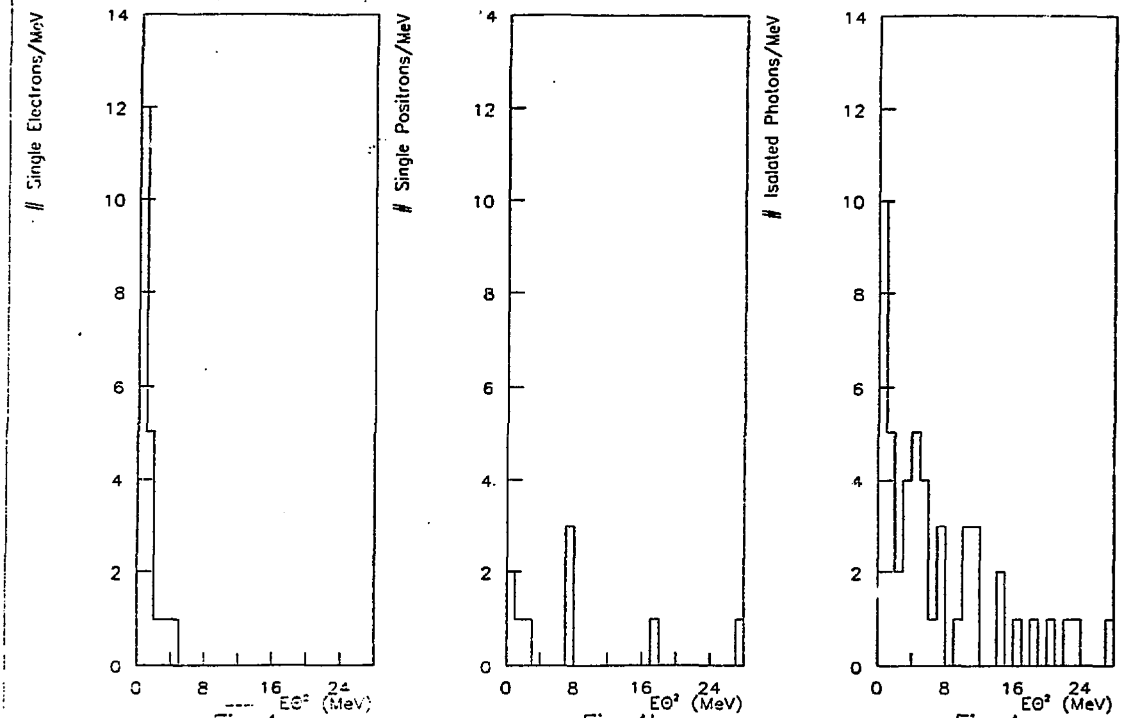

Fig. 4a Fig. 4b Fig. 4c

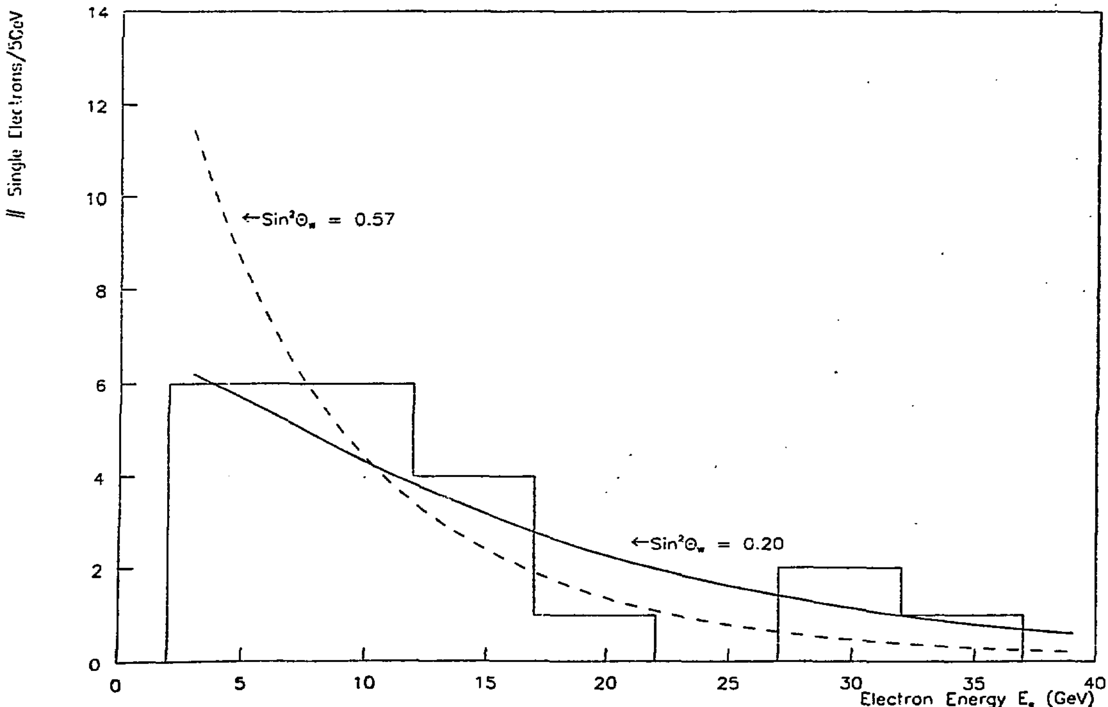

Fig. 5